ClassX Detection of Candidate Low-Luminosity Hard X-ray Binaries

A. A. Suchkov[1]& R. J. Hanisch[2]

STScI[3]

ABSTRACT

We present the results of a search for hard X-ray binaries (HXRBs) using the automated X-ray source classifier, *ClassX*, among the sources detected by *ROSAT* in PSPC pointed observations and listed in the White-Giommi-Angelini Catalog (WGACAT) as unidentified objects. Hard sources are defined as those with count rate ratios in the $0.9-2.0$ and $0.4-0.9$ keV bands greater than 10. Using ROSAT data and a flag indicating whether the source is known to be a radio source or not, *ClassX* identifies 35 new HXRB candidates, a number comparable to the 37 HXRBs previously identified in WGACAT. Almost all of the new candidate HXRBs are located within ± 2 deg of the Galactic plane, with substantial concentration toward the Galactic center. A number of them are seen in regions of obscuring nebulosity. They are on average much fainter and substantially softer than the known WGACAT HXRBs, and appear to represent a distinct low-luminosity population of hard low-mass X-ray binaries (LMXRB) associated with young stars.

Subject headings: methods: statistical — globular clusters: general — surveys — X-rays: general — X-rays: binaries — X-rays: stars

1. Introduction

The White-Giommi-Angellini Catalog (WGACAT) is a compilation of 76,763 sources detected in ROSAT PSPC pointed observations (http://wgacat.gfsc.nasa.gov). Less than 15% of the WGACAT sources have identifications. The identification and subsequent study of the remaining 85% of the sources would quite clearly have a profound impact on the understanding of the astrophysics of x-ray sources. To this end, we are using the *ClassX* automated classifier to determine the most likely identifications/object classes for the unidentified WGACAT sources. We report here on initial findings regarding hard X-ray binaries, where *ClassX* effectively doubles the number of HXRBs available for study.

2. HXRBs Identified by ClassX

We conducted a search for new HXRBs with the Web-based system for automated classification of X-ray sources *ClassX* (McGlynn et al. 2001, 2004, Suchkov et al. 2003). *ClassX* uses Virtual Observatory (VO) protocols[4] to collect the data necessary for classification from the world-wide network of online data

[1]suchkov@stsci.edu

[2]hanisch@stsci.edu

[3]Space Telescope Science Institute, operated by AURA Inc., under contract with NASA, 3700 San Martin Dr., Baltimore, MD 21218

[4]http://www.ivoa.net/

archives. It offers a variety of classifiers that can be used either individually or in combination to optimize classification for various object types.

In the current investigation we used a classifier that distinguishes eight classes of objects (QSOs, AGNs, galaxies, XRBs, white dwarfs, and hot, intermediate, and cool stars). The inputs to the classifier comprise X-ray data in four energy bands, positional information, and a flag indicating whether the X-ray source has a radio counterpart in the NVSS[5] or SUMSS[6] catalogs. The internal reliability (accuracy) with respect to classification of XRBs is $\approx 85\%$; reliability is noticeably higher for HXRBs, $\approx 94\%$. These reliability estimates were obtained using the previously identified WGACAT sources.

We characterize X-ray sources by the broad-band count rate,

$$C_{tot} = C(0.1 - 2.0), \tag{1}$$

'soft' count rate ratio,

$$R_0 = \frac{C(0.4 - 0.9)}{C(0.1 - 0.4)}, \tag{2}$$

and two 'hard' count rate ratios:

$$R_1 = \frac{C(0.9 - 2.0)}{C(0.4 - 0.9)} \tag{3}$$

and

$$R_2 = \frac{C(1.3 - 2.4)}{C(0.9 - 1.3)}, \tag{4}$$

where C is the count rate in the energy band shown in parentheses (in keV).

In the list of 67,470 unclassified WGACAT sources that have all the parameters required by the selected classifier (the list includes stars without spectral classification, which are considered here as unclassified), *ClassX* found 233 new XRB candidates (0.35% of the total number of sources). Of these, 35[7] (15%) are hard XRBs, $R_1 \geq 10$, (see Table 1). In comparison, there are 181 known XRBs out of the 9293 classified WGACAT sources (2%) of which 37 (20%) are HXRBs. The substantial difference in the fractions of XRBs in these two samples, 0.35% vs. 2%, is probably not surprising, in particular because XRBs are extremely bright X-ray objects and were looked for in very many previous studies. But the fractions of HXRBs in the two samples of XRBs are about the same, 15-20% of the total number of XRBs. As we discuss later, however, we must be cautious about drawing conclusions about any intrinsic similarities in these HXRB populations based on these simple counts.

Of 32 new candidate HXRBs, nine objects are in obscured regions and/or known OB associations and regions of active star formation. Two other objects are along sight lines to supernova remnants, including one which is to SN 386. Those in otherwise unremarkable stellar fields are all along the Galactic plane.

HXRBs have high energy spectra distinctly different from those of other X-ray sources. Because of that, *ClassX* easily differentiates them from other object types, isolating very reliable HXRB candidates. This is illustrated in Figure 1, which compares hard count rate ratios, R_1 and R_2, for hard X-ray sources, $R_1 \geq 10$,

[5]http://www.cv.nrao.edu/nvss/

[6]http://www.astrop.physics.usyd.edu/SUMSS/index.html

[7]Three sources classified as HXRB are, however, virtually indistinguishable in terms of their position and X-ray parameters, and should probably be considered as the same HXRB. Two more sources within 13″of each other may be in fact the same source.

identified in the WGACAT and by *ClassX* . It shows that the WGACAT and *ClassX* HXRBs have very similar $R_1 - R_2$ diagrams, which are at the same time conspicuously different from the same diagrams for other classes of objects. The difference is especially dramatic in the hardest part of the spectrum, where almost all *ClassX* HXRBs and most of the WGACAT HXRBs have $R_2 > 1.5$, while all the other classes of objects are located in the $R_1 - R_2$ diagram mostly below the line $R_2 = 1.5$.

Figure 2 shows the sky distributions of the *ClassX* HXRBs and compares it with that of the WGACAT HXRBs. The size of the data points is scaled by the source broad-band brightness that is defined, similar to the optical brightness, as $mx_{tot} = -2.5 \log C_{tot}$. This allows one to see that the HXRB candidates identified by ClassX are on average noticeably fainter than those classified as HXRBs in WGACAT. They are also softer, which is seen in Figure 3. These differences between the two samples are presented in a more quantified fashion in Figures 4 and 5. Figures 4 shows that the *ClassX* HXRBs are on average more than 10 times (in terms of total count rate) fainter. Such a difference might be due to larger distances and/or larger interstellar absorption. Indeed, Figure 2 shows that the new HXRBs are highly concentrated toward the Galactic plane, $b_{II} \sim \pm 2$ deg, and even more so toward the Galactic center, where absorption can be extremely high. However, comparison of the energy distributions of the *ClassX* and WGACAT HXRBs does not support the absorption hypothesis. Stronger absorption results in harder X-ray emission, but the new HXRB candidates, instead of being harder, are in fact on average substantially softer than the WGACAT HXRBs, by a factor of $\sim$2 in terms of count rate ratio R_0 (Figure 5). Therefore, the new HXRBs appear to be intrinsically fainter. This could be due to larger distances, though this seems unlikely. Given their strong concentration toward the Galactic plane and Galactic center larger distances would imply larger columns of absorbing material, which would again result in harder emission, contrary to the observations. We conclude, therefore, that the *ClassX* HXRBs differ from their WGACAT counterparts in two respects: they are on average intrinsically softer and less luminous.

3. Discussion

The known hard XRBs include both low-mass and high-mass XRBs (LMXRB and HMXRB, respectively), but the LMXRBs is the dominant specie; the same is probably true for the new HXRBs from ClassX. It appears that, as a group, hard XRBs may contribute substantially to understanding the origin of LMXRBs. The genesis of LMXRBs is often associated with globular clusters. Indeed, the fraction of low-mass XRBs per unit stellar luminosity in globular clusters is much higher than that in the field. Because of that, the field population is believed to be constituted primarily by XRBs ejected from globular clusters where they were originally formed (see, e.g., Sarazin et al. 2003 and references therein). This hypothesis may not work, however, for hard LMXRBs. Indeed, only one of the 37 hard XRBs previously known in the WGACAT, WGA J0042.2+4101, is in a globular cluster (located in M31); eight are known high-mass XRBs (HMXRB) and the rest are primarily Galactic LMXRBs in the field (a few sources have just a generic name XRB). Thus, none of the Galactic hard LMXRBs in the WGACAT sample is associated with globular clusters. This argues that, unlike the soft LMXRB population, the hard LMXRB population does not originate in globular clusters but rather is probably formed directly in the field. This inference is consistent with the strong concentration of hard XRBs toward the Galactic plane and the association of a few of them with regions of star formation. Indeed, this argues for very young age, whereas LMXRBs formed in globular clusters would have been extremely old and distributed throughout the bulge and the halo. The young age of the hard XRB population as a whole is also supported by the fact that, unlike globular clusters, which are very old, there are in the WGACAT HXRB sample a noticeable fraction of high-mass XRBs (eight out

of total 37), which are known to be very young.

Hard low-mass XRBs may shed new light on various phases of X-ray binary evolution. Taking into account intrinsically weaker X-ray emission of the *ClassX* HXRBs, one may infer that they are probably associated with the population of low-mass X-ray binaries in quiescence (see, e.g., Verbunt et al. 1994). In a more general context, the distinct population of HXRBs may provide a testbed for recent theories of evolution of low- and intermediate-mass XRBs. In particular, it seems to lend direct support to new populations of XRBs predicted by Podsiadlowski, Rappaport, & Pfahl (2002). These authors identified and modeled a large variety of XRB evolutionary channels, and argued that the "standard model" for the formation and evolution of XRBs is the exception rather than a rule. There was, however, a problem: the predicted median X-ray luminosities were too low when compared with those derived for well-observed systems. But now the newly identified *ClassX* HXRBs can substantially alleviate if not eliminate this predicament, providing the missing low-luminosity population required by the theory.

The ClassX HXRBs discussed above very much resemble a new class of wind-accreting neutron stars (WNS) predicted by Pfahl, Rappaport, & Podsiadlowski (2002). WNSs are believed to be hard, low-luminosity, young X-ray binaries, presumably accounting for the majority of the hard X-ray sources discovered by *Chandra*. It is likely that many or even most of the *ClassX* HXRBs are indeed young WNSs concentrated near the Galactic center and regions of star formation and representing the brighter part of the bulge population of numerous X-ray sources detected by *Chandra* (see Wang, Gotthelf, & Lang 2002). Given that HXRBs appear to be associated with young stars, there must be an overabundance of them in high-redshift galaxies, at the time when star formation rate was higher; locally, such an overabundance can be expected in starburst galaxies, and is probably associated with the rich population of x-ray point sources recently found in Chandra observations of starbursts (e.g., Soria & Wu 2003). If so, they can help to explain at least a part of the unexpectedly large number of "normal" galaxies among hard X-ray sources observed in deep *Chandra* surveys (see Moran, Fillipenko, & Chornock 2002 and references therein).

The authors wish to thank the ClassX team for ongoing support. RH thanks S. G. Neff for bringing to our attention a possible link between hard LMXRBs and the X-ray emission in starburst galaxies.

REFERENCES

McGlynn, T. et al. 2001, BAAS, 33, 1323

McGlynn, T. et al. 2004, ApJ, submitted

Moran, E. C., Filipenko, A. V., & Chornock, R. 2002, ApJ, 579, L71

Pfahl, E., Rappaport, S., & Podsiadlowski, Ph. 2002, ApJ, 571, L37

Podsiadlowski, Ph., Rappaport, S., & Pfahl, E. D. 2002, ApJ, 565, 1107

Sarazin, C. L., Kundu, A., Irwin, J. A., Sivakoff, G. R., Blanton, E. L., & Randall, S. W. 2003, ApJ, 595, 743

Soria, R. & Wu, K. 2003, A&A, 410, 53

Suchkov, A. A. & *ClassX* Team. 2003, in Astronomical Data Analysis Software and Systems XII, ASP Conf. Ser., Vol. 295, eds. H. F. Payne, R. I. Jedrzejewski, and R. N. Hook (San Francisco: ASP), 419

Verbunt, F., Belloni, T., Johnston, H.M., v.d. Klis, M., & Lewin, W.H.G. 1994, A&A, 285, 903

Wang, Q. D., Gotthelf, E. V., & Lang, C. C. 2002, Nature, 415, 148

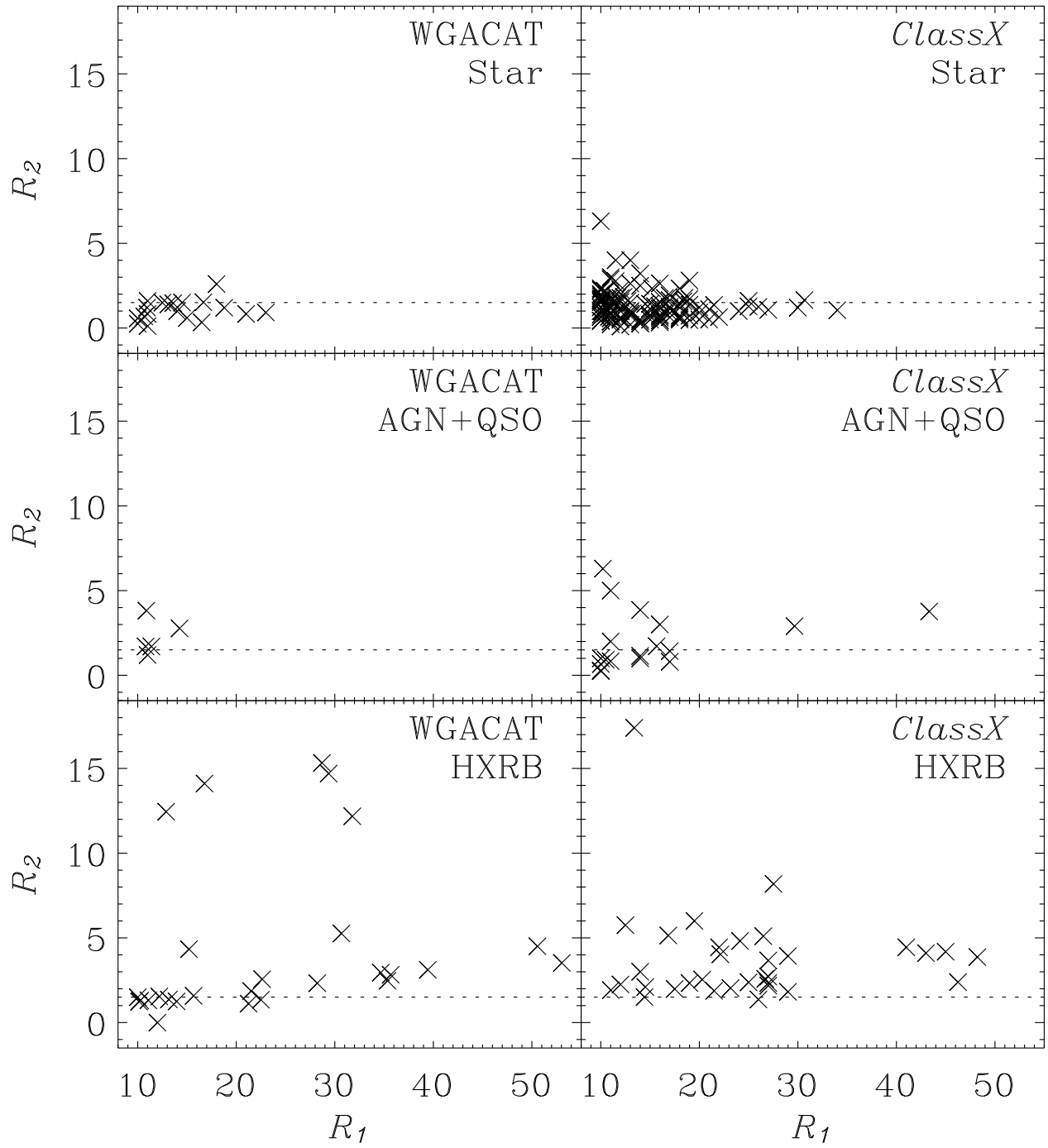

Fig. 1.— 'Hard' count rate ratios diagram for three classes of hard sources, $R_1 \geq 10$, identified in the WGACAT and by *ClassX* . The dotted line emphasizes that both WGACAT and *ClassX* HXRBs are harder than $R_2 = 1.5$ while stars and AGNs are generally softer.

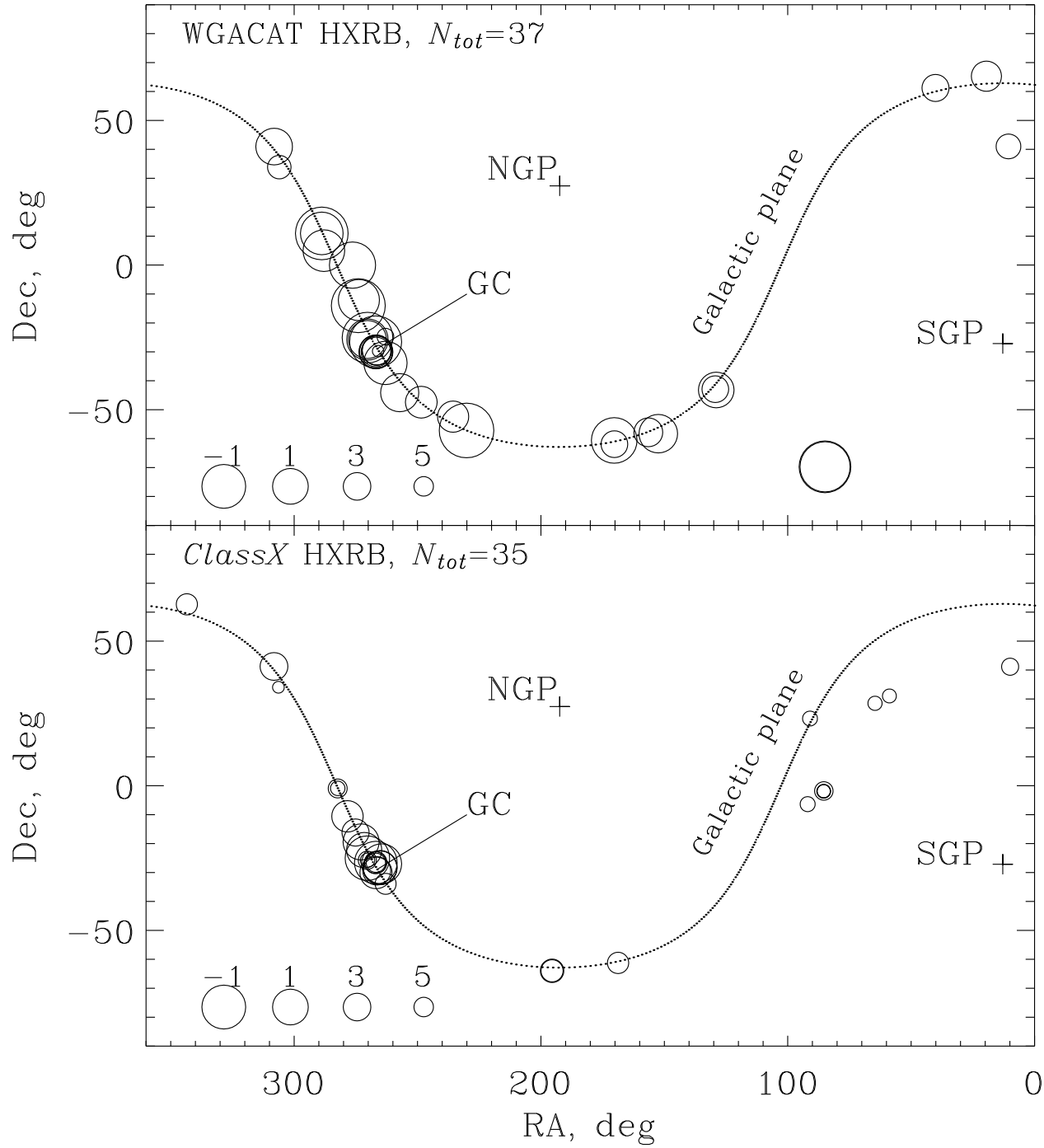

Fig. 2.— Sky distribution of the WGACAT and new *ClassX* HXRBs. The data point symbols are scaled with source $0.1 - 2.0$ keV brightness, $mx_{tot} = -2.5 \log C_{tot}$ (mag). Note that the *ClassX* sources are generally fainter than the previously known WGACAT sources.

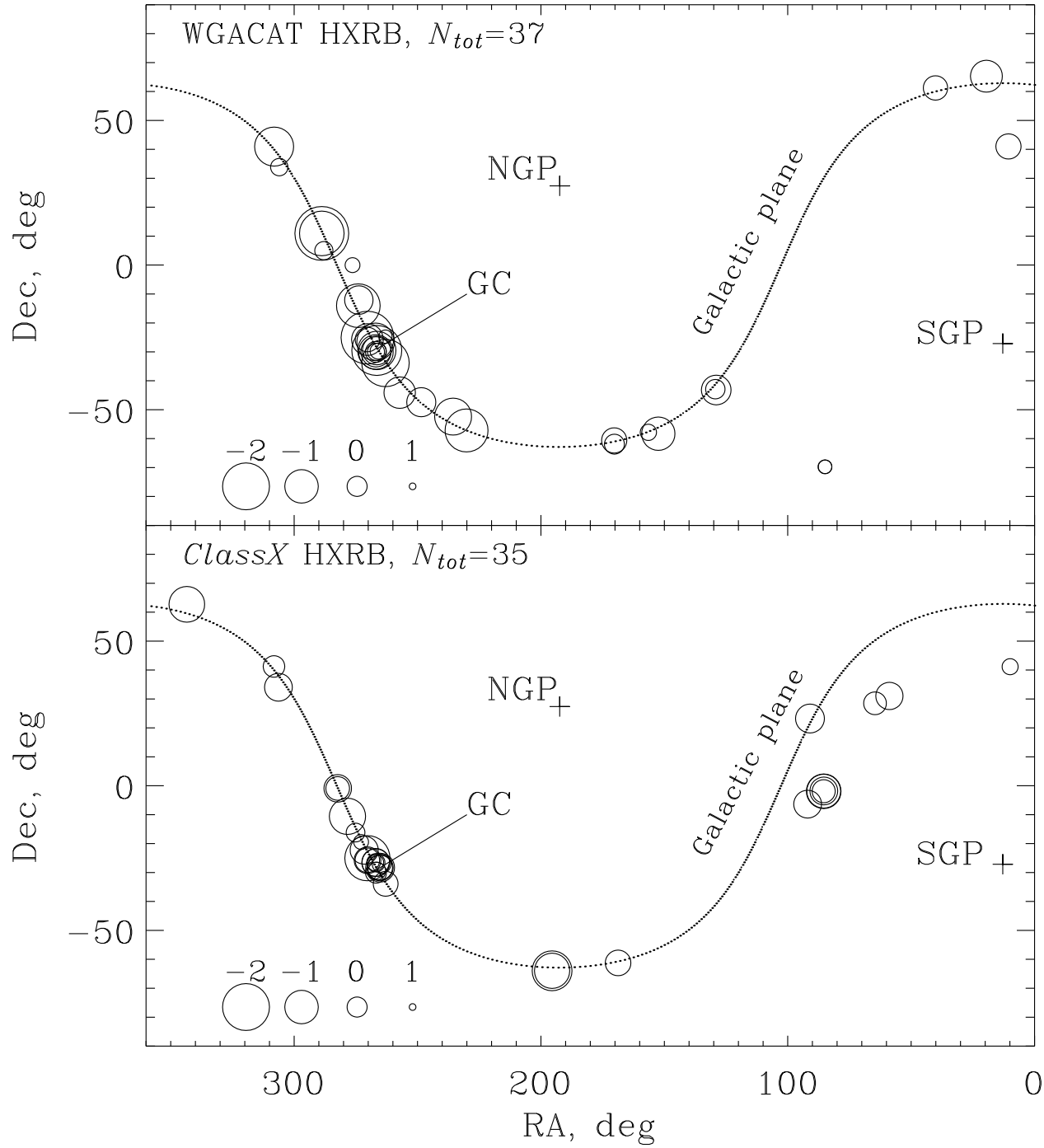

Fig. 3.— Same as in Figure 2 but the data point symbols are scaled with source X-ray 'color' that is defined as –2.5 log R_1 (mag), which is a measure of hardness in the *ROSAT* high-energy bands. Note that the ClassX sources are generally softer than the previously known WGACAT sources.

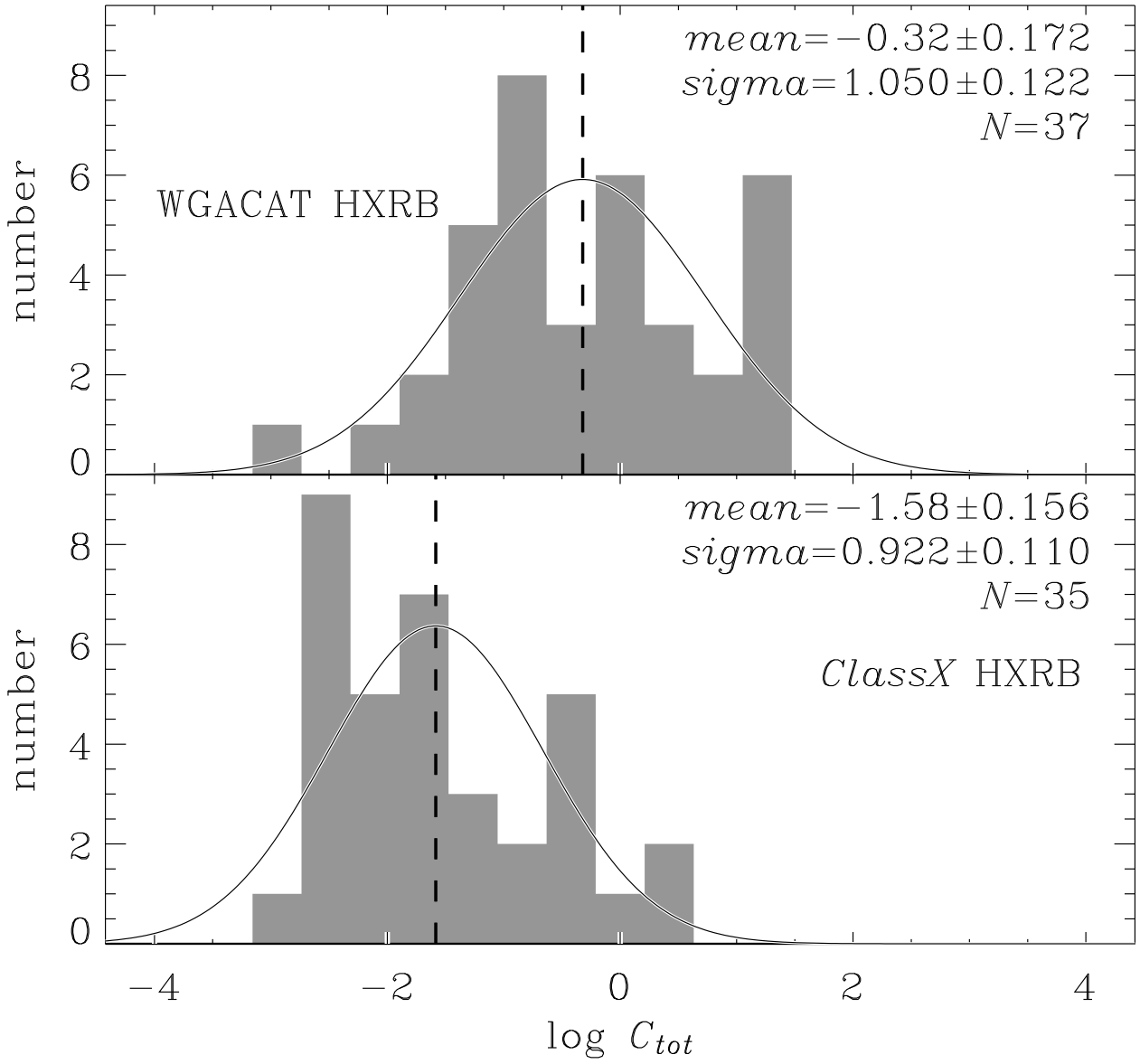

Fig. 4.— Total count rate distribution of HXRBs given in the WGACAT (upper panel) and identified by ClassX (lower panel). ClassX sources are on average fainter by $\log C_{tot} \sim 1.3$.

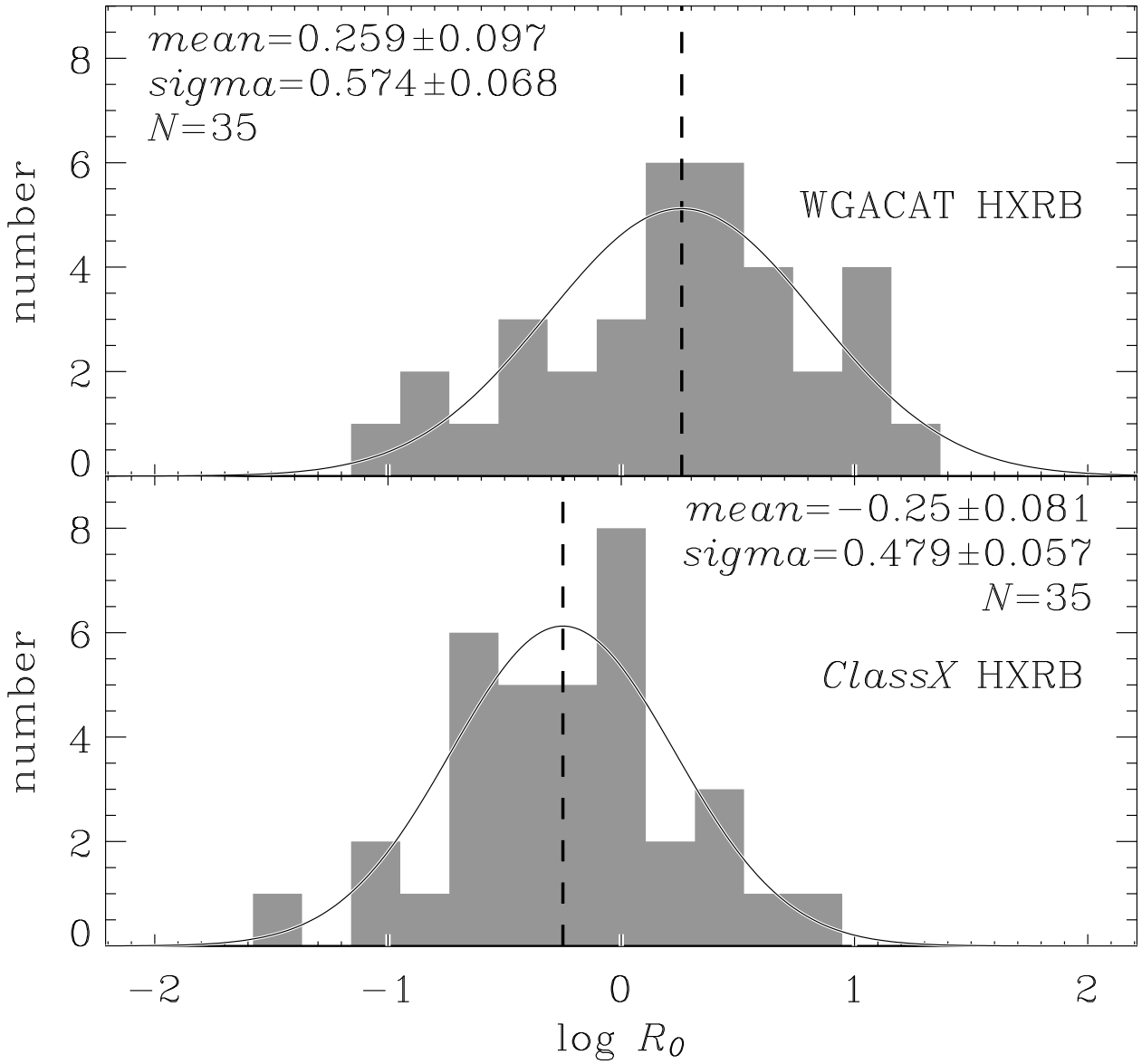

Fig. 5.— 'Soft' count rate ratio distribution of HXRBs given in the WGACAT and identified by ClassX. ClassX sources are on average softer by $\log R_0 \sim 0.5$.

Table 1. Hard XRB candidates identified by *ClassX*

WGACAT ID[a]	mx_{tot} mag	R_1	R_2	Comments
J0039.5+4109	5.5	12.0	2.2	stellar field, halo of M31
J0355.2+3102	6.3	26.0	1.3	stellar field; X Per=HD24534, known HMXRB, is 2.25 arcmin east
J0418.5+2830	6.3	19.0	2.3	V410 Tau 3' (var. star, Orion) to the south; sparse stellar field
J0541.5−0148	5.2	27.0	2.1	northern edge of NGC 2024 (Flame Nebula, in Orion)
J0541.6−0152	6.5	41.0	4.4	NGC 2024 (Flame Nebula, in Orion)
J0541.7−0154	6.4	43.0	4.0	NGC 2024 (Flame Nebula, in Orion)
J0541.7−0153	6.5	19.5	6.0	NGC 2024 (Flame Nebula, in Orion)
J0603.9+2314	6.1	29.0	1.8	stellar field; about 3 arcmin SW of 1 Gem=HD 41116, spec. binary
J0607.7−0621	6.1	27.0	2.7	Mon R2 HII region, SF region
J1114.9−6114	4.5	23.1	2.0	near NGC 3603, HII region, star formation region
J1301.9−6358	4.0	45.0	4.1	stellar field, near PSR1259−63
J1301.9−6357	4.3	61.7	4.2	stellar field, near PSR1259−63, only 15 from previous source
J1731.6−3353	4.6	22.0	4.4	stellar field; 4U1728−33 5 arcmin to NE, radio gal 5 arcmin to WNW
J1738.2−2659	−0.0	14.5	2.1	near Galactic center, in middle of RASS source
J1740.6−2818	1.4	24.1	4.8	Galactic center, RASS source
J1740.7−2818	1.4	29.0	3.9	same position as previous object
J1740.7−2817	1.4	22.1	4.0	same position as previous object
J1746.0−2929	2.9	13.4	17.0	near Galactic center, unremarkable field
J1747.3−3001	1.8	16.8	5.1	near Galactic center, unremarkable field
J1747.5−2637	5.0	14.0	3.0	near Galactic center, nothing special
J1747.6−2634	−0.7	26.6	2.5	same field as previous source
J1747.7−2629	4.3	27.0	3.6	same field as previous source
J1748.3−2635	4.3	12.5	5.7	adjacent to previous field
J1801.0−2544	6.2	25.0	2.3	stellar field
J1801.3−2502	−1.1	89.1	6.7	stellar field
J1801.3−2545	5.3	21.5	1.8	stellar field
J1806.4−2213	1.1	27.5	8.1	stellar field
J1811.4−1925	0.9	11.0	1.9	SN A.D. 386 = G11.2−0.3 at field center
J1820.4−1610	3.1	14.4	1.5	M17 HII region/cloud complex
J1833.5−1033	2.0	48.2	3.8	G21.5−0.90, Crab−like SNR
J1849.3−0053	6.2	26.5	5.0	stellar field, X-ray pos near 3C391
J1849.4−0055	5.1	20.2	2.5	stellar field, X-ray pos near 3C391
J2025.4+3403	6.9	27.0	2.3	stellar field, Cygnus
J2032.6+4114	2.9	17.5	1.9	stellar field, Cyg OB2 assoc.
J2253.9+6242	4.5	46.2	2.3	stellar field, Cep OB3 assoc.

[a]Prefix "WGA" in the source ID is omitted.